

## Quantum Phase Transition in a Two-Dimensional System of Dipoles

G. E. Astrakharchik,<sup>1</sup> J. Boronat,<sup>1</sup> I. L. Kurbakov,<sup>2</sup> and Yu. E. Lozovik<sup>2</sup>

<sup>1</sup>*Departament de Física i Enginyeria Nuclear, Campus Nord B4-B5, Universitat Politècnica de Catalunya, E-08034 Barcelona, Spain*

<sup>2</sup>*Institute of Spectroscopy, 142190 Troitsk, Moscow region, Russia*

(Received 10 August 2006; published 8 February 2007)

The ground-state phase diagram of a two-dimensional Bose system with dipole-dipole interactions is studied by means of a quantum Monte Carlo technique. Our calculation predicts a quantum phase transition from a gas to a solid phase when the density increases. In the gas phase, the condensate fraction is calculated as a function of the density. Using the Feynman approximation, the collective excitation branch is studied and the appearance of a roton minimum is observed. The results of the static structure factor at both sides of the gas-solid phase are also presented. The Lindemann ratio at the transition point becomes  $\gamma = 0.230(6)$ . The condensate fraction in the gas phase is estimated as a function of the density.

DOI: [10.1103/PhysRevLett.98.060405](https://doi.org/10.1103/PhysRevLett.98.060405)

PACS numbers: 05.30.Jp, 03.75.Hh, 64.60.-i, 71.10.Hf

The chromium atom has an exceptionally large permanent dipole moment, and the recent realization of Bose-Einstein condensation of  $^{52}\text{Cr}$  [1] has stimulated great interest in the properties of dipolar systems at low temperatures. It was observed [2] that dipolar forces lead to anisotropic deformation during expansion of the condensate. In the experiments [1,2], the dipolar forces were competing with short-range scattering. The latter, in principle, can be removed by tuning the  $s$ -wave scattering length to zero by Feshbach resonance [3]. This would lead to an essentially pure system of dipoles. On the other hand, low-dimensional systems can be realized by making the confinement in one (or two) directions so tight that no excitations of the levels of the tight confinement are possible and the system is dynamically two- (or one-) dimensional.

A major development has also been done in recent years towards the realization of excitons at temperatures close to the Bose-Einstein condensation temperature [4]. An exciton is much more stable if the electron is spatially separated from the hole (spatially separated excitons). Such an exciton can be modeled as a dipole. If the excitons are in two coupled quantum wells, they can be treated effectively as two-dimensional if the size of an exciton is small compared to the mean distance between excitons.

One might expect to find a phase transition from a gas phase to a crystal one at large density. As the condensate fraction is small at the transition point, perturbative theories, such as the Gross-Pitaevskii [5] or Bogoliubov [6,7] approaches, will fail to describe accurately this transition. One has to use *ab initio* numerical methods to address this quantum many-body problem. Recently, a trapped system of two-dimensional dipoles has been studied by the path integral Monte Carlo method [8], and the mesoscopic analog of crystallization has been found. Trapped dipoles with  $s$ -wave scattering were investigated [9]. So far, there have been no full quantum microscopic computations of the properties of a homogeneous system of dipoles.

The Hamiltonian of a homogeneous system of  $N$  bosonic dipoles has the form

$$\hat{H} = -\frac{\hbar^2}{2M} \sum_{i=1}^N \Delta_i + \frac{C_{\text{dd}}}{4\pi} \sum_{j < k} \frac{1}{|\mathbf{r}_j - \mathbf{r}_k|^3}, \quad (1)$$

where  $M$  is the dipole mass and  $\mathbf{r}_i$ ,  $i = \overline{1, N}$ , are the positions of dipoles. The expression for the coupling constant  $C_{\text{dd}}$  depends on the nature of the dipole-dipole interaction. Two possible physical realizations of a two-dimensional system of dipoles can be considered: (i) Cold atoms with permanent dipole moments  $m$  aligned perpendicularly to the plane of confinement by an external magnetic field. In this case,  $C_{\text{dd}} = \mu_0 m^2$ , where  $\mu_0$  is the permeability of free space. Alternatively, the electric dipole moment can be induced by an electric field  $E$ ; then the coupling constant is  $C_{\text{dd}} = E^2 \alpha^2 / \epsilon_0$ , where  $\alpha$  is the static polarizability and  $\epsilon_0$  is the permittivity of free space. (ii) Spatially indirect excitons. In two coupled quantum wells, one containing only holes and the other only electrons, holes and electrons might couple, forming indirect excitons. Another possible realization is a single quantum well where the exciton dipole moment is induced by a normal electric field. Spatial separation between the hole and the electron suppresses recombination and greatly increases the lifetime of an exciton. If the separation between excitons is greater than the electron-hole separation  $D$ , indirect excitons can be approximated as bosons with the dipolar moment oriented perpendicularly to the plane. In this case,  $C_{\text{dd}} = e^2 D^2 / \epsilon$ , where  $e$  is an electron's charge and  $\epsilon$  is the dielectric constant of the semiconductor. Study of 2D indirect exciton systems, in fact, is a hot topic, and this problem has been addressed both theoretically [10] and experimentally [4].

The Hamiltonian (1) can be written in dimensionless form by expressing all distances in units of characteristic length  $r_0 = MC_{\text{dd}} / (4\pi\hbar^2)$  and energies in units of  $\mathcal{E}_0 = \hbar^2 / Mr_0^2$ . Properties of a homogeneous system are governed

by the dimensionless parameter  $nr_0^2$  (dimensionless density), with  $n$  being density of the system.

In this Letter, we present a complete study of the phase diagram of two-dimensional bosonic particles with dipole-dipole interactions at zero temperature. We resort to the diffusion Monte Carlo (DMC) method [11] in order to find the ground-state energy and correlation functions of the many-body Hamiltonian (1). Within the DMC method, the Schrödinger equation is solved in imaginary time for the product of the ground-state wave function and a trial (or guiding) wave function, which we chose to be of the Bijl-Jastrow form:  $\Psi_T(\mathbf{r}_1, \dots, \mathbf{r}_N) = \prod_{i=1}^N f_1(\mathbf{r}_i) \prod_{j < k}^N f_2(|\mathbf{r}_j - \mathbf{r}_k|)$ . In the gas phase, the density profile is constant and  $f_1(r) = \text{const}$ . When two particles closely approach, the influence of other particles can be neglected, and we expect that  $f_2(\mathbf{r})$  is well approximated by the solution of the two-body scattering problem. We choose the short distance part of the two-body correlation term as  $f_2(r) = C_1 K_0(2/\sqrt{r})$ , where  $K_0(r)$  is a modified Bessel function of the second kind and  $C_1$  is some constant. At large distances, instead, the contribution from other particles must not be neglected, and collective behavior (phonons) is expected. From hydrodynamic theory, it was shown [12] that in a two-dimensional system the phononic long-range part of the wave function decays as  $f_2(r) \propto \exp(-\text{const}/r)$ . We use this functional dependence in a symmetrized form  $f_2(r) = C_2 \exp(-C_3/r) \times \exp[-C_3/(L-r)]$ , which ensures that  $f_2'(L/2) = 0$ . We match the short- and long-range parts of  $f_2(r)$  and demand continuity of the function and its first derivative at a matching distance  $R_{\text{match}}$ . This, together with the condition  $f_2(L/2) = 1$ , fixes constants  $C_1$ ,  $C_2$ , and  $C_3$ . In the solid phase, we use the same  $f_2(r)$  and add the one-body Gaussian localization term  $f_1(r_i) = \exp[-\alpha(\mathbf{r}_i - \mathbf{r}_i^{\text{cr}})^2]$ ,  $i = \overline{1, N}$ , where  $\alpha$  is the localization strength and  $r_i^{\text{cr}}$  is the position of the lattice site. Variational parameters  $R_{\text{match}}$  and  $\alpha$  are chosen by minimizing the variational energy.

We model the homogeneous system at density  $n$  by considering  $N$  particles in a simulation box with periodic boundary conditions. The size of the box  $L_x \times L_y$  is chosen in such a way that  $n = N/(L_x L_y)$ . In the gas phase, a square box  $L_x = L_y$  is considered, while in the solid phase we ensure that each of the box sides is a multiple of an elementary cell size in a triangular lattice.

The advantage of the DMC method is that it gives essentially exact energy within some statistical uncertainties. In a system of dipoles, special attention should be paid to an appropriate extrapolation to the infinite system. The reason for that is that, while the  $1/r^3$  dipole-dipole interaction is not yet a long-range one in a two-dimensional system [13], the long-range decay is already quite slow. The finite-size effects in energy can be significantly reduced by adding the *tail* energy

$$\frac{E_{\text{tail}}(n, L)}{N} = \frac{1}{2} \int_{L/2}^{\infty} V(r) g_2(r) 2\pi r dr \quad (2)$$

to the output of the DMC calculation with  $L = \min\{L_x, L_y\}$ . Here  $V(r)$  is the interaction potential and  $g_2(r)$  is the pair distribution function. An approximate value of the integral (2)  $E_{\text{tail}}/N = C_{\text{dd}} n^{3/2}/(2\sqrt{N})$  is obtained by substituting  $g_2(r)$  by its average value in the bulk  $g_2(r) = n$ . This greatly suppresses finite-size dependence (for the example shown in the inset in Fig. 1, by a factor of 25), while the residual dependence is eliminated by a fitting procedure. We note that the dependence on the number of particles in this case scales as  $1/\sqrt{N}$ , contrary to the law  $1/N$ , usual for fast decaying potentials. We do the extrapolation of the energy  $E(N) = E_{\text{DMC}} + E_{\text{tail}}$  to the thermodynamic limit value  $E_{\text{th}}$  using as fitting formula:  $E(N) = E_{\text{th}} + C/N^{1/2}$ , where  $C$  is a fitting constant. In the inset in Fig. 1, we show an example of the finite-size study for the energy. In it, we consider a density  $nr_0^2 = 256$  and a solid phase, where we expect to find the largest finite-size dependence, due to the oscillatory behavior of the pair distribution function. We find that our fitting function describes well the finite-size dependence, and we use it for the extrapolation to the thermodynamic limit. The same procedure is repeated for densities  $nr_0^2 = 32, 48, 64, 96, 128, 196, 256, 384, 512, 768$ , and 1024 and for the gas and solid phases.

In Fig. 1, we show the results of the ground-state energy for gas and solid phases. We find that at small density the gas phase is energetically favorable and the solid phase is metastable. At larger densities, the system crystallizes and a triangular lattice is formed. We fit our data points with a dependence  $E/N = a_1(nr_0^2)^{3/2} + a_2(nr_0^2)^{5/4} + a_3(nr_0^2)^{1/2}$ , where the powers 3/2 and 5/4 describe the proper asymp-

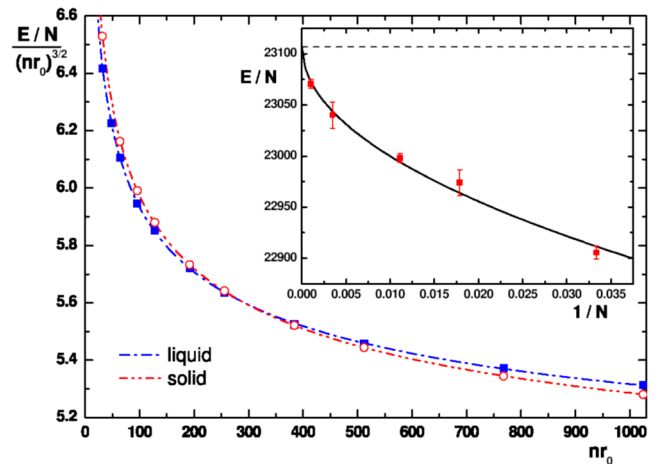


FIG. 1 (color online). Energy per particle of the dipole system as a function of the dimensionless density  $nr_0^2$ : (blue) solid squares, gas phase; (red) open circles, solid phase. Energy is measured in units  $[\hbar^2/(Mr_0^2)]/(nr_0^2)^{3/2}$ . Inset: An example of the finite-size dependence for the energy in the solid phase at dimensionless density  $nr_0^2 = 256$ ; symbols, DMC energy [with added tail energy, Eq. (2)]; solid line, fit  $E_{\text{th}} + C/\sqrt{N}$ ; dashed line, extrapolation of the energy to infinite system size  $E_{\text{th}}$ . Energy in the inset is measured in units of  $\hbar^2/(Mr_0^2)$ .

otic behavior of potential and kinetic energies, respectively, and the power 1/2 is added for a better accuracy of the fit. The best parameters of the fit are  $a_1 = 4.536(8)$ ,  $a_2 = 4.38(4)$ , and  $a_3 = 1.2(3)$  for the gas phase and  $a_1 = 4.43(1)$ ,  $a_2 = 4.80(3)$ , and  $a_3 = 2.5(2)$  for the solid. The transition is estimated to happen at the critical density  $nr_0^2 = 290(30)$ . We note that in a one-dimensional system the role of interactions is enhanced and the transition happens at much smaller densities  $nr_0 \approx 0.4$  [14]. Maxwell double tangent construction shows that the region of phase coexistence is very small, and freezing and melting points are indistinguishable within the error bars of our calculation. At large densities, quantum fluctuations get suppressed, and the energy is dominated by the potential energy of particle-particle interactions. The energy eventually approaches the limit of a classical crystal. The triangular lattice in this limit has potential energy  $E_{\text{triang}}/N = 4.446(nr_0)^{3/2}$ .

Knowledge of the equation of state  $E(n)/N$  of a homogeneous system permits the calculation of the chemical potential  $\mu(n) = \partial E/\partial N$  and the speed of sound  $c: Mc^2 = n\partial\mu/\partial n$ . This information is extremely useful for the description of trapped systems with a large number of particles. As is well known, the local density approximation can be used for predictions of the density profile, release energy, frequencies of collective modes, etc., which can be accessed in experiments [15].

We estimate the thermodynamic Lindemann ratio  $\gamma = \sqrt{\langle(\mathbf{r} - \mathbf{r}^c)^2\rangle}/a_L$  ( $a_L$  is the lattice length), at the transition density as  $\gamma = 0.230(6)$ . Comparing to other two-dimensional systems, we find that this value is smaller than the one of a hard disk  $\gamma = 0.279$ , while it is similar to more long-ranged potentials, such as  $\gamma = 0.235(15)$  for Yukawa bosons and  $\gamma = 0.24(1)$  for Coulomb bosons [16]. In a three-dimensional system, the value of  $\gamma$  at the transition is generally larger; for example,  $\gamma = 0.28$  for the Yukawa potential [17].

The breaking of translational symmetry takes place in the crystal. Periodic modulation appears in the density profile  $n(r)$  and the pair correlation function  $g_2(r - r') = \langle n(r)n(r') \rangle$ . We have studied the static structure factor  $S_k$  which is related to  $g_2(r)$  by Fourier transformation  $S_k = 1 + 2\pi \int_0^\infty [g_2(r) - n] J_0(kr) r dr$ . We use a technique of pure estimators which essentially removes any bias from a particular choice of the guiding wave function [18]. The static structure factor increases from zero at  $k = 0$  to unity for large momentum. In the gas phase,  $S_k$  increases smoothly and has a peak around inverse interparticle distance  $n^{1/2}$  (see Fig. 2). As the dimensionless density  $nr_0^2$  is increased, the correlations get stronger and the height of the peak is increased. In the solid phase, the static structure factor is discontinuous and has a  $\delta$ -function peak at inverse lattice site length  $a_L^{-1} = (\sqrt{3}n/2)^{1/2} = 0.93 \dots n^{1/2}$ .

We can get some insight on the excitation spectrum  $E_k$  by relating it to the static structure factor through the Feynman relation

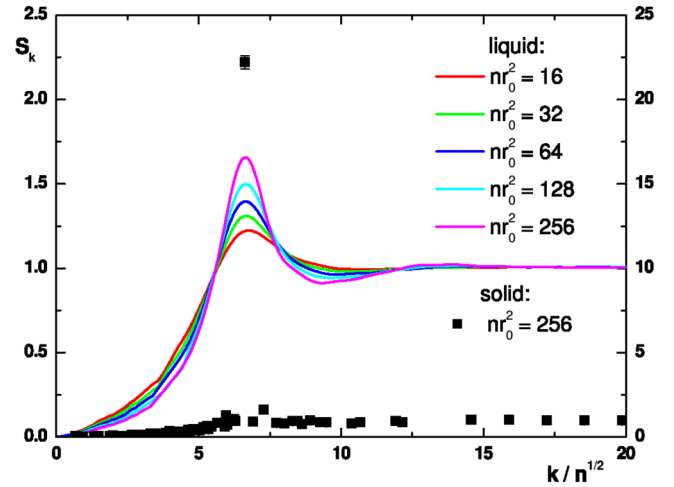


FIG. 2 (color online). Static structure factor: left axis, gas phase at densities  $nr_0^2 = 16, 32, 64, 128,$  and  $256$  (the higher the peak, the larger the density); right axis, solid phase at density  $nr_0^2 = 256$ .

$$E_k = \frac{\hbar^2 k^2}{2MS_k}. \quad (3)$$

This relation is expected to be exact for small momenta (i.e., in the phononic regime), while at larger momenta it gives an upper bound to the excitation spectrum [19]. Predictions for  $E_k$  obtained from DMC data are presented in Fig. 3. We find that deviations from low-momenta phononic linear behavior appear very soon. The excitation spectrum is monotonous for the smallest considered density. As the density increases, the roton minimum at a finite value of the momentum is observed (see also Ref. [7]). The roton gap  $\Delta$  decreases as the density is increased. We expect that our approach gives the correct position of the roton minimum, while the real value of the roton gap  $\Delta$  is

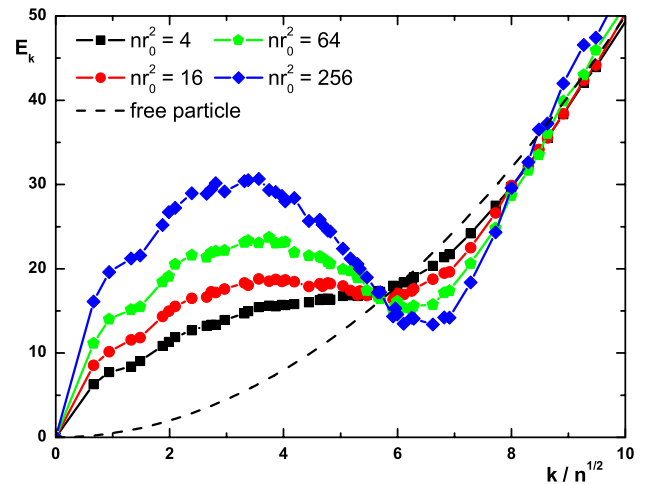


FIG. 3 (color online). Upper bound for the excitation spectrum in the gas phase. Solid lines, Feynman formula—Eq. (3)—applied to the DMC data for the static structure factor; dashed line, free particle limit. Energy is measured in units of  $\hbar^2/(Mr_0^2)$ .

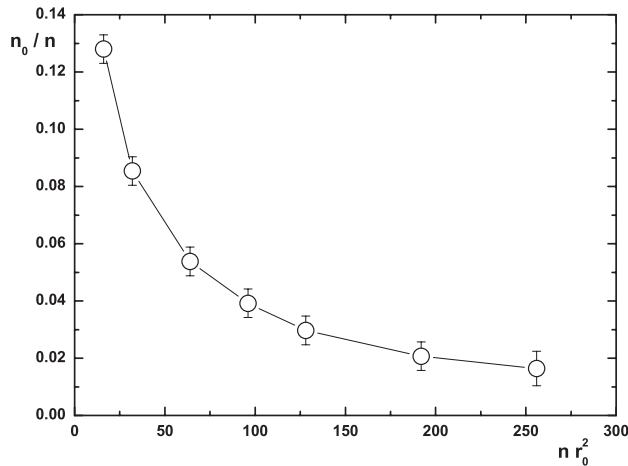


FIG. 4. Condensate fraction as a function of the dimensionless density  $nr_0^2$ .

overestimated, as happens in DMC calculations for gas helium [20].

While Bose-Einstein condensation is expected to happen in dilute systems, strong interactions between particles destroys coherence. In order to study the process of decoherence quantitatively, we measure the condensate density  $n_0$ . In a homogeneous system, it can be found from the long-range asymptotic  $|r - r'| \rightarrow \infty$  of the one-body density matrix (OBDM)  $g_1(r - r') = \langle \hat{\Psi}^\dagger(r) \hat{\Psi}(r') \rangle$ , where  $\hat{\Psi}(r)$  is the field operator. As  $g_1(r)$  is a nonlocal quantity, the DMC output gives for it a *mixed* estimator, which is biased by the choice of the guiding function. This bias can be significantly diminished by the extrapolation procedure [18]. We have measured asymptotics of OBDM for different sizes of the system and made extrapolation to the thermodynamic limit. In Fig. 4, we plot the condensate fraction as a function of the dimensionless density in the gas phase. We find that the condensate depletion is large in the range of considered densities. This prohibits the use of the perturbative Bogoliubov approach for prediction of the condensate depletion and justifies the necessity of a numerical approach to the problem. The condensate fraction is rather small at the transition density.

In conclusion, we have investigated the zero-temperature quantum phase diagram of a two-dimensional dipole system and estimated the critical density of the gas to solid phase transition. We studied structural properties by observation of the pair distribution function, static structure factor, and Lindemann ratio. Coherence properties are investigated by looking at the one-body density matrix. The condensate fraction decreases rapidly with the density and is estimated to be very small (2%) at the transition point. Our predictions can be checked in future experiments with spatially separated indirect excitons and cold dipolar Bose gases in reduced geometry.

After completion of this work, we became aware of Ref. [21], in which systems of  $N = 36, 90$  dipoles are studied by the finite-temperature path integral MC method with a result for  $n_c$  compatible with our prediction.

Some of the authors (G. E. A. and J. B.) acknowledge support by (Spain) Grant No. FIS2005-04181 and Generalitat de Catalunya Grant No. 2005SGR-00779. The work was partially supported by RFBR.

- 
- [1] A. Griesmaier *et al.*, Phys. Rev. Lett. **94**, 160401 (2005).  
 [2] J. Stuhler *et al.*, Phys. Rev. Lett. **95**, 150406 (2005).  
 [3] J. Werner *et al.*, Phys. Rev. Lett. **94**, 183201 (2005).  
 [4] A. A. Dremin *et al.*, JETP Lett. **76**, 450 (2002); R. Rapaport *et al.*, Phys. Rev. Lett. **92**, 117405 (2004); L. V. Butov *et al.*, *ibid.* **92**, 117404 (2004); V. V. Krivolapchuk *et al.*, Phys. Rev. B **64**, 045313 (2001).  
 [5] P. M. Lushnikov, Phys. Rev. A **66**, 051601(R) (2002); L. Santos *et al.*, Phys. Rev. Lett. **85**, 1791 (2000).  
 [6] D. H. J. O'Dell, S. Giovanazzi, and C. Eberlein, Phys. Rev. Lett. **92**, 250401 (2004).  
 [7] D. H. J. O'Dell, S. Giovanazzi, and G. Kurizki, Phys. Rev. Lett. **90**, 110402 (2003); L. Santos, G. V. Shlyapnikov, and M. Lewenstein, *ibid.* **90**, 250403 (2003).  
 [8] Yu. E. Lozovik, S. Y. Volkov, and M. Willander, JETP Lett. **79**, 473 (2004).  
 [9] K. Nho and D. P. Landau, Phys. Rev. A **72**, 023615 (2005); D. C. E. Bortolotti *et al.*, cond-mat/0604432.  
 [10] Yu. E. Lozovik *et al.*, JETP **44**, 389 (1976); JETP Lett. **22**, 274 (1975); **64**, 573 (1996); Phys. Lett. A **228**, 399 (1997); Phys. Rev. B **59**, 5627 (1999); **66**, 075124 (2002); O. L. Berman *et al.*, *ibid.* **70**, 235310 (2004); S. Conti *et al.*, *ibid.* **57**, R6846 (1998); M. A. Olivares-Robles *et al.*, *ibid.* **64**, 115302 (2001); S. I. Shevchenko, Phys. Rev. Lett. **72**, 3242 (1994); X. Zhu *et al.*, *ibid.* **74**, 1633 (1995); S. De Palo *et al.*, *ibid.* **88**, 206401 (2002).  
 [11] For a general reference on the DMC method, see, e.g., J. Boronat and J. Casulleras, Phys. Rev. B **49**, 8920 (1994).  
 [12] L. Reatto and G. V. Chester, Phys. Rev. **155**, 88 (1967).  
 [13] In a 2D system, the long-range interaction should decay slower than  $1/r^2$ ; see, for example, *Dynamics and Thermodynamics of Systems with Long-Range Interactions*, edited by T. Dauxois *et al.* (Springer, Berlin, 2002).  
 [14] A. S. Arkhipov *et al.*, Pis'ma Zh. Eksp. Teor. Fiz. **82**, 41 (2005) [JETP Lett. **82**, 39 (2005)].  
 [15] G. E. Astrakharchik, Phys. Rev. A **72**, 063620 (2005).  
 [16] L. Xing, Phys. Rev. B **42**, 8426 (1990); W. R. Magro and D. M. Ceperley, Phys. Rev. B **48**, 411 (1993); Phys. Rev. Lett. **73**, 826 (1994).  
 [17] D. Ceperley, G. V. Chester, and M. H. Kalos, Phys. Rev. B **17**, 1070 (1978).  
 [18] J. Casulleras and J. Boronat, Phys. Rev. B **52**, 3654 (1995).  
 [19] J. Boronat *et al.*, Phys. Rev. B **52**, 1236 (1995).  
 [20] J. Boronat and J. Casulleras, Europhys. Lett. **38**, 291 (1997).  
 [21] H. P. Büchler *et al.*, preceding Letter, Phys. Rev. Lett. **98**, 060404 (2007).